PAPER

Check for updates

Fine-tuning of radiative properties by "mild" substituents: searching for a perfectly soft chromophore†

Grażyna Orzanowska,[a] Claudia Ryppa,[b] Mathias O. Senge [ID] *[b] and Jacek Waluk [ID] *[ac]

Controlling spectral properties to achieve desired characteristics is an attractive goal in application-oriented research, *e.g.*, in the design of fluorescence sensors. "Soft" chromophores, molecules with strong spectral responses to internal or external perturbations are good candidates for such studies. In this work, absorption, fluorescence, and magnetic circular dichroism (MCD) spectra were obtained for a series of porphyrins, substituted at the meso-positions with n-hexyl groups. As the number of substituents increases from 1 to 4, significant changes are observed. The intensity of the S_0-S_1 transition (Q_x) in the 0–0 region strongly decreases in mono-substituted porphyrin, but upon additional substitutions it increases to values larger than in the parent, unsubstituted molecule. Such behavior can be explained, using the perimeter model, by changes in the energy splittings between the two highest (HOMO) and two lowest (LUMO) frontier molecular orbitals. Single substitution makes porphyrin a nearly perfect soft chromophore, but upon introduction of a larger number of n-hexyl groups it is transformed into a hard one. DFT simulations incorrectly predict a continuous transition from a soft to hard chromophore, because the calculated ordering of two HOMO orbitals is opposite to that obtained by experiment. On the other hand, for those porphyrins that can be classified as hard chromophores, the calculations nicely reproduce contributions of Franck–Condon and Herzberg–Teller terms to absorption and fluorescence spectra.

Introduction

Rational design of materials considered for applications based on light–matter interactions requires a detailed spectral and photophysical characterization of a potentially useful chromophore. One of the crucial parameters in this respect is the radiative constant of the S_0-S_1 electronic transition (k_r).

[a] *Institute of Physical Chemistry, Polish Academy of Sciences, Kasprzaka 44/52, 01-224 Warsaw, Poland. E-mail: jwaluk@ichf.edu.pl*

[b] *School of Chemistry, Chair of Organic Chemistry, Trinity Biomedical Sciences Institute, Trinity College Dublin, The University of Dublin, 52-160 Pearse Street, Dublin D02R590, Ireland*

[c] *Faculty of Mathematics and Science, Cardinal Stefan Wyszyński University, Dewajtis 5, 01-815 Warsaw, Poland*

† Electronic supplementary information (ESI) available: Description of computational procedures, atomic coordinates obtained for optimized geometries, calculated orbital energy splittings, orbital parentage of the lowest energy singlet state, rates of nonradiative and nonradiative depopulation of S_1; comparison of experimental and calculated energies for Q and Soret transition, comparison of absorption and MCD spectra simulated using BP86-D and INDO/S methods, comparison of experimentally measured absorption with the simulated ones that take into account both FC and HT contributions. See DOI: https://doi.org/10.1039/d4cp01502a

The value of k_r determines the strength of the absorption; it also competes with k_{nr}, the sum of the rate constants of processes responsible for nonradiative S_1 depopulation. Since the fluorescence quantum yield is proportional to k_r, maximizing its value is particularly important for generating efficient fluorophores. This can be achieved, *e.g.*, by substitution that enhances k_r. Quite often, however, such modifications involve strongly electron donating or withdrawing moieties and may lead to undesired changes, such as decrease of photostability. Therefore, a chemically "mild" substituent that would affect the radiative properties of a chromophore without changing the other characteristics is an attractive solution.

A simple and very useful procedure that allows predicting a spectral response of a cyclic π-electron system to substitution is based on the perimeter model.[1] A chromophore of interest is derived from an ideal [n]annulene perimeter by perturbations that may include various effects, *e.g.*, substitution by an electron withdrawing or accepting group. Analytical formulas have been derived that allow predictions of spectral changes caused by a specific perturbation from the knowledge of energy splittings in the two pairs of frontier orbitals: two highest occupied (HOMO) and two lowest unoccupied (LUMO) ones. The magnitude of the

17944 | *Phys. Chem. Chem. Phys.*, 2024, **26**, 17944–17950

This journal is © the Owner Societies 2024

splitting can be readily evaluated by inspection of the shapes of the orbitals of the parent perimeter.

The perimeter model points to the class of compounds for which, upon substitution, one can expect large changes in the electronic parameters that characterize electronic absorption, emission, as well as magnetic circular dichroism.[1] These compounds belong to the category of the so-called "soft" chromophores, characterized by similar or, at best, equal values of the energy differences between the frontier π orbitals: two highest occupied (ΔHOMO) and two lowest unoccupied ones: (ΔLUMO). For such systems, dramatic effects can be observed, *e.g.*, changes of MCD signs upon single substitution with an "innocuous" methyl group, as reported for methyl-substituted pyrenes.[2]

Transition from a soft (ΔHOMO $\approx$ ΔLUMO) to a hard (ΔHOMO $\gg$ ΔLUMO or ΔHOMO $\ll$ ΔLUMO) chromophore often results in a large increase of radiative parameters. This has been predicted[3] and experimentally demonstrated for porphyrin[4–13] and its isomers.[14–16] The "hardest" among the isomers is porphycene, whereas parent porphyrin ('porphine') is a soft chromophore. The differences in the orbital energy patterns result in the S_1(0–0) absorption in porphycene being about 50 times stronger than in porphyrin.[17]

The frontier orbitals energy pattern in porphyrin does not exactly correspond to an ideal soft chromophore, for which ΔHOMO = ΔLUMO. The present and previous[18] DFT calculations, consistent with the observed MCD signs, indicate that HOMO orbitals are split by a small amount, whereas the LUMOs are nearly degenerate, and therefore ΔHOMO > ΔLUMO. One can therefore ask whether, by using appropriate substitution, it is possible to get closer to equal HOMO and LUMO splittings. In this work, we test this possibility by investigating spectroscopic and photophysical properties of the parent porphyrin and five derivatives bearing 1, 2, 3, and 4 n-hexyl groups at the meso-positions (Fig. 1). Alkyl groups act as weak electron donors, which means that they mostly interact with HOMO orbitals, raising their energy. The effect depends on the value of the linear combination of atomic orbitals (LCAO) coefficient at the position of substitution in a particular porphyrin orbital. Two scenarios are possible, depicted in Fig. 2. If the lower occupied frontier orbital (HOMO−1) has a node at the meso-position, the destabilization of the other (HOMO) orbital will lead, upon successive substitutions, to monotonic increase of ΔHOMO, making the chromophore harder and harder. For the opposite orbital ordering the situation is more complicated. The initial substitution may decrease
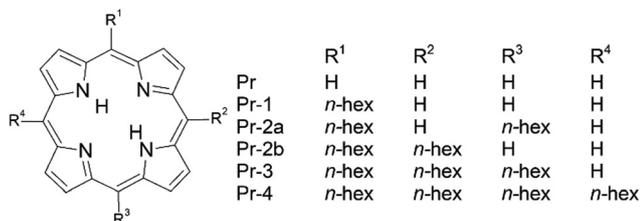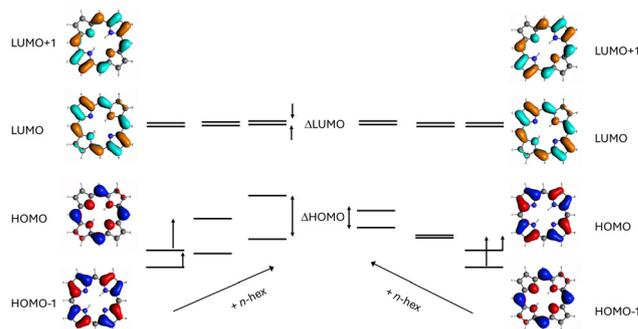

Fig. 2 Changes of orbital energies upon substitution with alkyl groups as expected for two possible orderings of HOMO energy levels.

the energy gap, but once the ordering is inverted, ΔHOMO will increase. In this work, we demonstrate for n-hexyl substituted porphyrins, that the latter case occurs. Depending on the number of substituents, the parent porphyrin can be transformed into a nearly perfect soft or a hard chromophore. In contrast, nonradiative properties of the S_1 state remain practically unchanged. We also show how the ratio of Franck–Condon and Herzberg–Teller contributions to the probability of weakly allowed S_0–S_1 and S_0–S_2 transitions evolves when a chromophore passes from soft to hard regime.

Materials and methods

Syntheses of **Pr**, **Pr-1**,[19] **Pr-2a**, **Pr-2b**,[20] **Pr-3**,[21] and **Pr-4**[22] have been reported before.

Absorption spectra were measured on Shimadzu UV-3100 and UV-2700 spectrophotometers. Fluorescence spectra were recorded with an Edinburgh FS 090 CDT spectrofluorometer. The same apparatus was used for fluorescence decay measurements, with a 370 nm, 1.5 ns pulse NanoLED (IBH) as the excitation source. FAST software package (Edinburgh Instruments) was used for the determination of decay times. Fluorescence quantum yields were obtained using cresyl violet in ethanol (φ_{fl} = 0.55)[23] and porphycene in n-hexane (φ_{fl} = 0.44)[24] as references.

Magnetic circular dichroism (MCD) spectra were initially measured with an OLIS DSM17 spectropolarimeter equipped with a $\approx$1 T permanent magnet, and then remeasured on a JASCO J-1500 spectropolarimeter, for which the magnetic field of the electromagnet was calibrated using the MCD signal of aqueous $CoSO_4$ solution[25] as a standard (nominal field value of 1.5 T, 1.36 T after calibration).

Spectroscopic grade solvents (Merck, UVASOL) have been used. n-Hexane solutions were studied in most cases, except for the parent, unsubstituted porphyrin, for which, due to solubility problems, toluene was used for absorption and MCD studies in the low energy region and for the determination of absorption coefficients.

Quantum-chemical calculations were applied to simulate absorption and MCD spectra. Electronic transition energies were initially calculated using time-dependent density functional

Fig. 1 Structural formulas of the porphyrins investigated.

	R^1	R^2	R^3	R^4
Pr	H	H	H	H
Pr-1	n-hex	H	H	H
Pr-2a	n-hex	H	n-hex	H
Pr-2b	n-hex	n-hex	H	H
Pr-3	n-hex	n-hex	n-hex	H
Pr-4	n-hex	n-hex	n-hex	n-hex

This journal is © the Owner Societies 2024

Phys. Chem. Chem. Phys., 2024, **26**, 17944–17950 | **17945**

theory (TDDFT) with Gaussian 03[26] (B3LYP/6-31G(d,p)). Next, the calculations were extended to include MCD, as implemented in the ADF software package.[27] BP86-D functional with DZP basis set were used; similar combinations were successful in the analysis of electronic spectra of porphyrinoids.[28–30] In all cases, geometry optimization was performed prior to calculating transition energies.

For **Pr-2b**, two 'trans' tautomeric forms are possible; we label them **Pr-2b′** and **Pr-2b″**. Calculations performed for both tautomers indicate that they are nearly isoenergetic and that their spectral properties should be very similar.

In addition to DFT-based methods, calculations were also done using an extended version of DZDO, an INDO/S-based program, kindly provided by Josef Michl and John Downing.

Results

Absorption spectra

The absorption spectra of all the investigated compounds (Fig. 3) exhibit the pattern typical for porphyrins.[31] Four main bands are observed in the low energy region, corresponding to two lowest electronic transitions, $L_1(Q_x)$ and $L_2(Q_y)$. For both L_1 and L_2, the lower energy part corresponds mainly to the 0–0

Fig. 3 Comparison of absorption spectra of the porphyrins studied (*n*-hexane solutions at 293 K, toluene for **Pr**).

transition; it is followed by a stronger band, which contains vibronic contributions. Very intense Soret band,[32] observed in the blue region contains at least two electronic transitions (B_1 and B_2). Inspection of Fig. 3 shows that the introduction of consecutive *n*-hexyl moieties leads to pronounced spectral changes. The Soret band gradually shifts to the red and becomes more intense. The behavior of Q bands is less regular. All four bands gradually shift to lower energies, but the intensity changes for 0–0 transitions are very different from those of the vibronic components. The latter are not much affected by the substitution. On the contrary, intensities of 0–0 transitions exhibit dramatic and non-monotonous changes. Upon single *n*-hexyl substitution, going from **Pr** to **Pr-1**, the 0–0 band practically disappears for Q_x and becomes extremely weak for the Q_y transition. Adding more substituents, however, results in the gradual increase of the 0–0 band intensity. In **Pr-4**, this effect is so strong that the intensity of the $S_1(0–0)$ band becomes higher than that of the vibronic component. Similarly, the two bands contributing to Q_y become comparable in intensity: the intensity ratio (measured at the band maximum) is 0.79, compared to 0.18 in unsubstituted **Pr** and 0.12 in **Pr-1**.

Fluorescence spectra

Comparison of the fluorescence spectra (Fig. 4) reveals trends similar to those observed in absorption. The relative intensity of the 0–0 band strongly varies across the series: as in absorption, it is the highest in **Pr-4** and lowest in **Pr-1**. The spectra of the two doubly substituted porphyrins are very similar, which suggests additive, relative position-independent contributions from the substituents. Analogous behavior is observed in absorption, as revealed by comparison of the spectra of **Pr-2a** and **Pr-2b**.

The fluorescence quantum yield (Table 1) varies along the series. The lowest emission intensity is observed for **Pr-1**, whereas **Pr-4** shows the highest values. Fluorescence quantum yields of **Pr-2a**, **Pr-2b**, and **Pr** are practically the same. Comparison of the emission spectral profiles shows that the monotonic increase in the quantum yield upon passing from **Pr-1** to **Pr-4** is due to the growing intensity of the 0–0 region, whereas the vibronic part remains practically unchanged. Such behavior reflects the trend observed in absorption.

No changes in the fluorescence lifetime (τ) could be observed. All the measured values are in the range of 7.8–8.1 ns and are considered to be the same within experimental error. Since the fluorescence quantum yields are rather low, this observation indicates that the rates of nonradiative S_1 depopulation (Table S2, ESI†), which govern the decay time, do not change with substitution. In contrast, the emission quantum yields scale with k_r, since $\varphi_{fl} = k_r \times \tau$.

MCD spectra

All the investigated porphyrins exhibit the same pattern of MCD signs: −, +, −, + for the L_1, L_2, B_1, and B_2 transitions (Fig. 5). According to the perimeter model, such a sequence corresponds to $\Delta HOMO > \Delta LUMO$. The signals in the low energy region are much weaker than for the Soret bands. Most
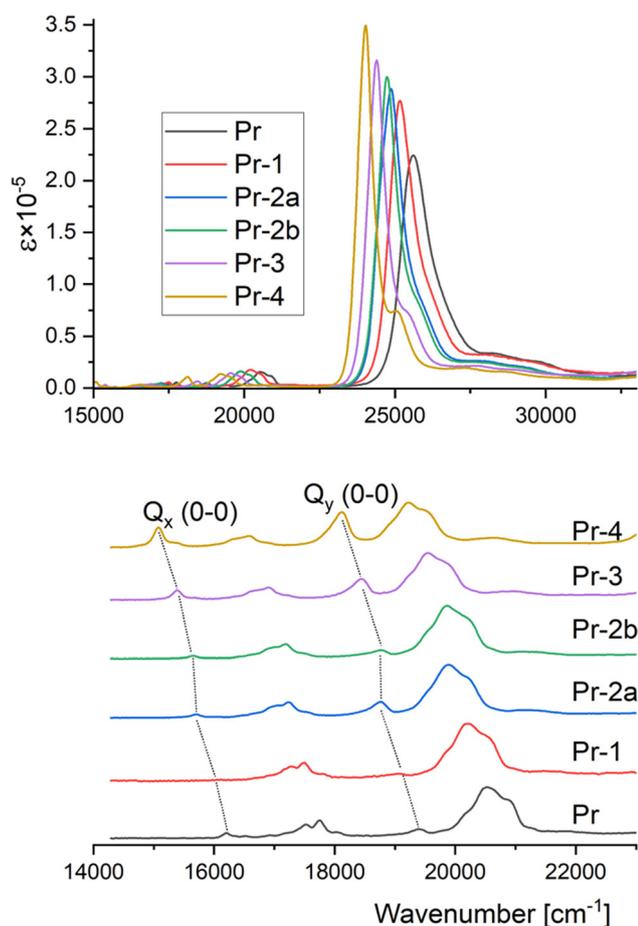
17946 | *Phys. Chem. Chem. Phys.*, 2024, **26**, 17944–17950
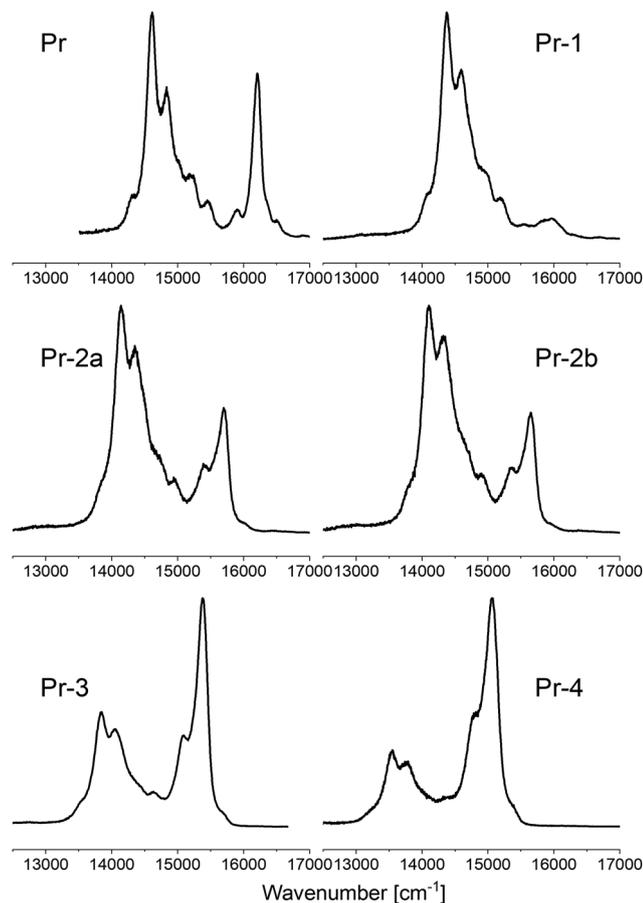
This journal is © the Owner Societies 2024

Fig. 4 Comparison of fluorescence spectra for **Pr** and hexyl-substituted porphyrins (*n*-hexane solutions at 293 K).

Table 1 Fluorescence quantum yields and lifetimes (293 K, *n*-hexane solutions)

	$\varphi_{fl}{}^{a}$	$\tau_{fl}{}^{b}$ [ns]
Pr	0.027^{c}	7.9
	0.044^{d}	11.1^{d}
Pr-1	0.021	7.9
Pr-2a	0.025	7.8
Pr-2b	0.027	7.8
Pr-3	0.035	7.8
Pr-4	0.042	8.1

^{a} Estimated accuracy: $\pm 20\%$. ^{b} ± 0.2 ns. ^{c} Estimated value. ^{d} Toluene solution.

Fig. 5 Comparison of MCD spectra for the porphyrins studied (*n*-hexane solutions at 293 K, except for **Pr**, for which absorption and MCD in the low energy range were measured in toluene, and for the $S_1(0-0)$ transition in **Pr-1** measured in dichloromethane).

interesting is the intensity ratio of the 0–0 transitions in Q_x and Q_y to the corresponding vibronic bands. A similar pattern as in absorption and fluorescence spectra is observed. The $S_1(0-0)$ transition is extremely weak in **Pr-1**, but introduction of consecutive *n*-hexyl moieties leads to its large increase with respect to the vibronic counterpart, so that it becomes dominant in **Pr-3** and **Pr-4**. A similar behavior is observed for S_2. It is noteworthy that the $S_1(0-0)$ transition in **Pr-1** is unique with respect to its positive MCD sign, since all other compounds display negative MCD signals for this transition. In contrast, **Pr-1** is no
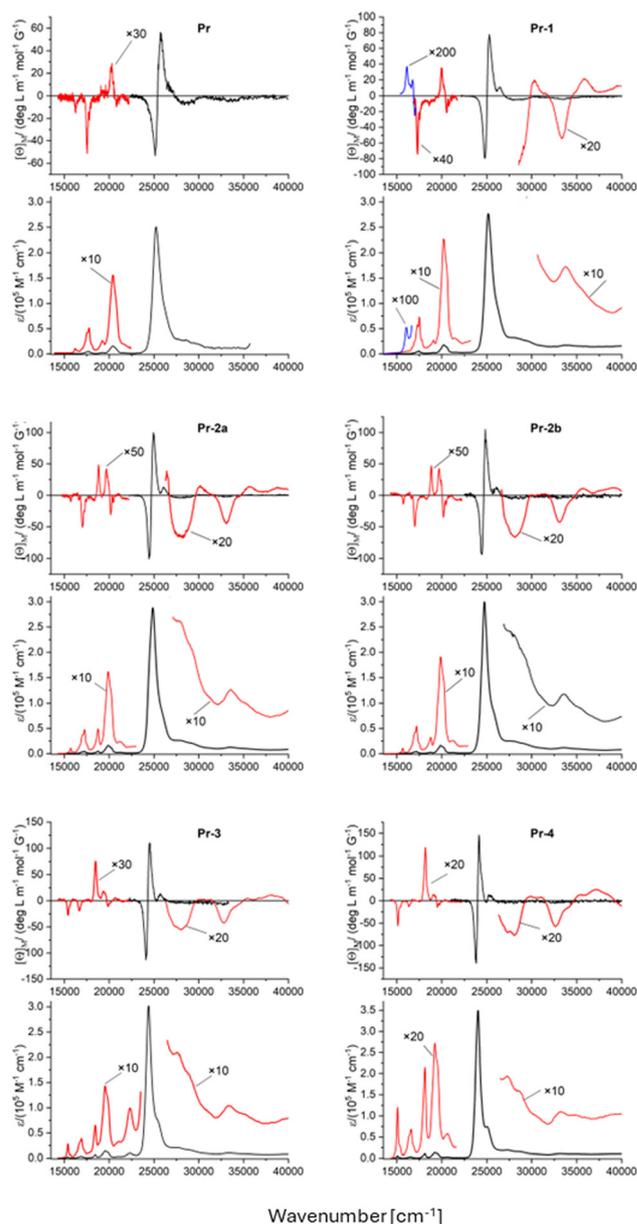
exception regarding the vibronic features of S_1, revealing the same negative sign as all other porphyrins investigated.

Calculations

It has been established that, in order to properly describe the weak S_0-S_1 (Q_x) transition in free base porphyrin, two contributions have to be taken into account: Franck–Condon (FC) and Herzberg–Teller (HT). The former is responsible for the 0–0 region, whereas the HT terms are dominant in the vibronic features that form the second band, stronger in both absorption and emission. The Q_x band served as the case study in theoretical works that included both Herzberg–Teller and

This journal is © the Owner Societies 2024

Phys. Chem. Chem. Phys., 2024, **26**, 17944–17950 | **17947**

Duschinsky effects.[33,34] The spectra could be reproduced very well by calculations.

Our present results clearly show that the perturbation of the porphyrin macrocycle by the *meso*-substitution strongly affects the FC intensity, whereas the HT contributions remain approximately constant. This is observed in the three types of spectra that we recorded: absorption (Fig. 3), fluorescence (Fig. 4), and MCD (Fig. 5). All show (for both Q_x and Q_y bands) significant changes in the intensity ratio of the 0–0 band with respect to the vibronic features. The 0–0 region is very sensitive to substitution, whereas the intensity of the vibronic bands remains approximately constant. Interestingly, the changes are not monotonic: the first substitution leads to a decrease of FC *vs.* HT contributions, but upon introducing two or more *n*-hexyl groups, the intensity in the 0–0 region steadily grows. In the perimeter model, this implies that the ΔHOMO $-$ ΔLUMO difference decreases upon passing from **Pr** to **Pr-1**, and then continuously increases. Such behavior is compatible with the orbital energy ordering shown in the right part of Fig. 2. However, both B3LYP and BP86-D DFT functionals used in this work predict the other sequence. Therefore, they are unable to reproduce the decrease of 0–0 band intensity in **Pr-1** with respect to **Pr**. Instead, they predict continuous growth concomitant with the increasing number of substituents (Fig. S2–S7, ESI†). On the other hand, lower intensity in **Pr-1** than in **Pr** is correctly predicted by INDO/S (Fig. S2 and S3, ESI†). This is because of the calculated energy ordering of the frontier occupied orbitals, opposite to that predicted by DFT, which agrees with the experimental findings. In turn, the INDO/S method fails to reproduce the intensity increase starting from double substitution: the calculated $S_1 \leftarrow S_0$ oscillator strengths start growing in **Pr-3**, but even for **Pr-4** they are lower that the value computed for **Pr** (Fig. S4–S7, ESI†).

The difficulty in predicting the sign of ΔHOMO $-$ ΔLUMO in a soft chromophore has been discussed before.[35] In line with the present results, inversion of MCD signs observed for several substituted zinc porphyrins was correctly predicted by INDO/S, but not DFT calculations. The problem is caused by similar HOMO-1 and HOMO energies (difference of about 0.1 eV). Fortunately, the splitting of LUMO and LUMO+1 in all presently studied porphyrins is even lower (0.02–0.04 eV), so that all DFT calculations yield ΔHOMO $>$ ΔLUMO, the ordering that agrees with the experimentally observed pattern of MCD signs for Q and Soret transitions. The only exception is the positive MCD observed for an extremely weak 0–0 band of **Pr-1** (Fig. 5), a molecule which is the closest to an ideal soft chromophore.

The experimentally observed transition energy shifts to the red with the increasing number of substituents are well predicted by both DFT models (Fig. 6). The general trend in absorption intensity changes is also well reproduced, except for **Pr-1**, as discussed above.

Simulations of absorption and fluorescence spectra were performed using the algorithm proposed in the case study of porphyrin, now implemented in Gaussian.[33] This allowed a comparison of FC and HT contributions along the series (Fig. 6). The calculations predict a monotonic increase of FC
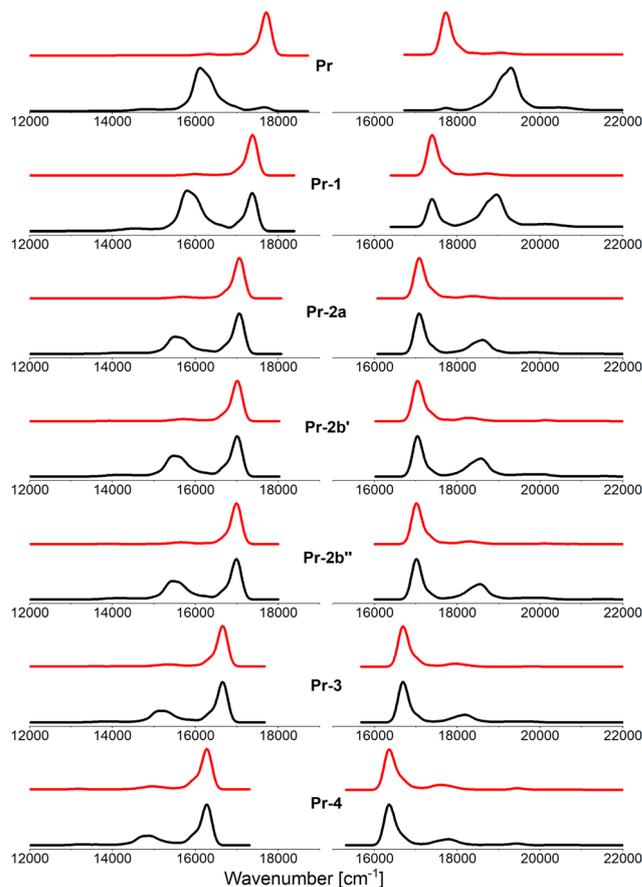

Fig. 6 Calculated FC (top, red) and FCHT (bottom, black) spectra, normalized to the maximum, convoluted with a Gaussian of 135 cm^{-1} width (FWHM). Right, absorption, left, fluorescence.

intensity in the 0–0 region with respect to the vibronic bands that mainly consist of HT induced contributions. Except for **Pr-1**, the agreement with experiment is good (Fig. S8–S13, ESI†), especially for **Pr-3** and **Pr-4**, molecules which exhibit the largest ΔHOMO $-$ ΔLUMO values and are therefore the hardest chromophores along the series.

We have also simulated the MCD spectra, using DFT (BP86-D functional) and INDO/S (Fig. S2–S7, ESI†). Similar patterns as in the absorption calculations were obtained. The sign sequence was computed correctly by both models (except from INDO/S calculations for L_1 and L_2 in **Pr-3** and **Pr-4**), but the intensity changes were not. DFT predicted continuous MCD increase of Q_x and Q_y MCD intensities along the series, whereas INDO/S correctly reproduced the decrease upon passing from **Pr** to **Pr-1**, but the experimentally observed increase for the growing number of *n*-hexyl moieties was not predicted. However, INDO/S fared much better in the Soret region, for which DFT calculations predicted a number of transitions located lower than the Soret bands; weak in absorption, but closely spaced. This proximity of states led to several calculated strong MCD signals with intensity similar to that of the Soret transitions. Such pattern is not observed experimentally (Fig. 5). In contrast, in agreement with the experiment, INDO/S calculations correctly

17948 | *Phys. Chem. Chem. Phys.*, 2024, **26**, 17944–17950

This journal is © the Owner Societies 2024

predicted that the MCD is dominated by two strong signals from the Soret bands.

Discussion and conclusions

The experimental results, obtained by using three different techniques, reveal a characteristic pattern of spectroscopic evolution with the increasing number of alkyl substituents. The observed changes in absorption, fluorescence, and MCD spectra can be readily interpreted based on the simple, but powerful perimeter model. Unsubstituted porphyrin, a soft chromophore, comes very close to be an ideal case of ΔHOMO = ΔLUMO upon a single substitution with an alkyl residue. Adding more substituents leads to ΔHOMO > ΔLUMO with a continuous increase of the difference in orbital energy splittings. In other words, depending on the number of substituents, a soft chromophore can be made either softer or harder. One should note that these changes influence not only the transition intensities, but the color of absorbed or emitted light, because of different responses of FC and HT to substitution. Thus, fluorescence becomes more light red in **Pr-3** and **Pr-4** due to the increasing FC contribution in the 0–0 region.

The computational results demonstrate that a proper calculation of orbital energy ordering remains a challenge when the orbitals lie close to each other. As shown for unsubstituted **Pr**, different methods can predict different orderings. Thus, it would be instructive to check various DFT functionals in this regard.

Approaching an ideal soft chromophore *via* electron-donating substitution has an alternative. If an electron withdrawing group is used, it will mostly interact with one of the LUMO orbitals, increasing the ΔLUMO gap. In a sense, the situation is then simpler than that involving HOMO orbitals. Since the two LUMOs are nearly degenerate, a perturbation will increase the splitting for each of both possible orbital energy orderings.

One can think of diverse applications for a perfectly soft chromophore. It should be extremely sensitive to small environmental effects, thus being a good candidate for an optical sensor. Usually, such devices are based on signal intensity changes. We note that, because of different responses of FC and HT contributions to external perturbations, working in ratiometric mode should be possible. In addition, not only the intensity, but also the spectral profile and, in the case of MCD, the sign of the signal can be changed. Therefore, (possibly very small) changes in the vicinity of the chromophore could be probed by different spectral techniques, increasing the measurement accuracy and sensitivity of such a device.

An ideal soft chromophore could also be very helpful in theoretical studies of vibronic effects in electronic transitions. An example of a problem that calls for deeper analysis is provided by the MCD spectrum of **Pr-1**, which reveals, for the same $S_1 \leftarrow S_0$ electronic transition, opposite signs in the 0–0 and vibronic regions.

Finally, we would like to underscore the validity of simple models to understand phenomena which cannot be correctly treated by models that formally are considered more developed. In the present work, using only DFT for spectral predictions leads to inconsistencies between experiment and theory. On the other hand, the perimeter model not only explains the observed spectral changes well, but also gives an understanding of why DFT calculations fail in certain cases.

Conflicts of interest

There are no conflicts to declare.

Acknowledgements

Notes and references

1 J. Michl, Magnetic Circular-Dichroism of Aromatic-Molecules, *Tetrahedron*, 1984, **40**, 3845–3934.

2 J. Waluk and J. Michl, Determination of Positional Isomers of Methylpyrenes and Other Polycyclic Hydrocarbons by Magnetic Circular Dichroism, *Anal. Chem.*, 1981, **53**, 236–239.

3 J. Waluk and J. Michl, The perimeter model and magnetic circular dichroism of porphyrin analogues, *J. Org. Chem.*, 1991, **56**, 2729–2735.

4 J. D. Keegan, A. M. Stolzenberg, Y. C. Lu, R. E. Linder, G. Barth, A. Moscowitz, E. Bunnenberg and C. Djerassi, Magnetic circular dichroism studies. 60. Substituent-induced sign variation in the magnetic circular dichroism spectra of reduced porphyrins. 1. Spectra and band assignments, *J. Am. Chem. Soc.*, 1982, **104**, 4305–4317.

5 J. D. Keegan, A. M. Stolzenberg, Y. C. Lu, R. E. Linder, G. Barth, A. Moscowitz, E. Bunnenberg and C. Djerassi, Magnetic circular dichroism studies. 61. Substituent-induced sign variation in the magnetic circular dichroism spectra of reduced porphyrins. 2. Perturbed molecular orbital analysis, *J. Am. Chem. Soc.*, 1982, **104**, 4317–4329.

6 C. Djerassi, Y. Lu, A. Waleh, A. Y. L. Shu, R. A. Goldbeck, L. A. Kehres, C. W. Crandell, A. G. H. Wee, A. Knierzinger, R. Gaeteholmes, G. H. Loew, P. S. Clezy and E. Bunnenberg, Magnetic Circular-Dichroism Series. 65. Sign Variation in the Magnetic Circular-Dichroism Spectra of Free-Base Porphyrins Having a Single Pi-Acceptor Pyrrole Ring Substituent – Structure Implications, *J. Am. Chem. Soc.*, 1984, **106**, 4241–4258.

7 R. A. Goldbeck, B. R. Tolf, E. Bunnenberg and C. Djerassi, Substituent conformational effects in the magnetic circular

This journal is © the Owner Societies 2024

Phys. Chem. Chem. Phys., 2024, **26**, 17944–17950 | **17949**

dichroism and absorption spectra of free-base carbonyl porphyrins, *J. Am. Chem. Soc.*, 1987, **109**, 28–32.

8 A. Gorski, M. Kijak, E. Zenkevich, V. Knyukshto, A. Starukhin, A. Semeikin, T. Lyubimova, T. Roliński and J. Waluk, Magnetic Circular Dichroism of meso-Phenyl-Substituted Pd-Octaethylporphyrins, *J. Phys. Chem. A*, 2020, **124**, 8144–8158.

9 A. Ceulemans, W. Oldenhof, C. Görller-Walrand and L. G. Vanquickenborne, Gouterman's "four-orbital" model and the MCD spectra of high-symmetry metalloporphyrins, *J. Am. Chem. Soc.*, 1986, **108**, 1155–1163.

10 R. A. Goldbeck, Sign variation in the magnetic circular dichroism spectra of π-substituted porphyrins, *Acc. Chem. Res.*, 1988, **21**, 95–101.

11 N. Kobayashi and K. Nakai, Applications of magnetic circular dichroism spectroscopy to porphyrins and phthalocyanines, *Chem. Commun.*, 2007, 4077–4092.

12 J. Mack, M. J. Stillman and N. Kobayashi, Application of MCD spectroscopy to porphyrinoids, *Coord. Chem. Rev.*, 2007, **251**, 429–453.

13 H. M. Rhoda, J. Akhigbe, J. Ogikubo, J. R. Sabin, C. J. Ziegler, C. Brückner and V. N. Nemykin, Magnetic Circular Dichroism Spectroscopy of meso-Tetraphenylporphyrin-Derived Hydroporphyrins and Pyrrole-Modified Porphyrins, *J. Phys. Chem. A*, 2016, **120**, 5805–5815.

14 J. Waluk, M. Müller, P. Swiderek, M. Köcher, E. Vogel, G. Hohlneicher and J. Michl, Electronic states of porphycenes, *J. Am. Chem. Soc.*, 1991, **113**, 5511–5527.

15 A. Gorski, E. Vogel, J. L. Sessler and J. Waluk, Magnetic circular dichroism of octaethylcorrphycene and its doubly protonated and deprotonated forms, *J. Phys. Chem. A*, 2002, **106**, 8139–8145.

16 A. Gorski, E. Vogel, J. L. Sessler and J. Waluk, Magnetic circular dichroism of neutral and ionic forms of octaethylhemiporphycene, *Chem. Phys.*, 2002, **282**, 37–49.

17 J. Waluk, Spectroscopy and tautomerization studies of porphycenes, *Chem. Rev.*, 2017, **117**, 2447–2480.

18 H. Cortina, M. L. Senent and Y. G. Smeyers, Ab initio comparative study of the structure and properties of H_2-porphin and H_2-phthalocyanine. The electronic absorption spectra, *J. Phys. Chem. A*, 2003, **107**, 8968–8974.

19 A. Wiehe, C. Ryppa and M. O. Senge, A Practical Synthesis of Meso-monosubstituted, β-Unsubstituted Porphyrins, *Org. Lett.*, 2002, **4**, 3807–3809.

20 S. Hatscher and M. O. Senge, Synthetic access to 5,10-disubstituted porphyrins, *Tetrahedron Lett.*, 2003, **44**, 157–160.

21 S. Horn and M. O. Senge, The Intermolecular Pauson–Khand Reaction of meso-Substituted Porphyrins, *Eur. J. Org. Chem.*, 2008, 4881–4890.

22 A. Wiehe, Y. M. Shaker, J. C. Brandt, S. Mebs and M. O. Senge, Lead structures for applications in photodynamic therapy. Part 1: Synthesis and variation of m-THPC (Temoporfin) related amphiphilic A_2BC-type Porphyrins, *Tetrahedron*, 2005, **61**, 5535–5564.

23 J. Olmsted III, Calorimetric Determinations of Absolute Fluorescence Quantum Yields, *J. Phys. Chem.*, 1979, **83**, 2581–2584.

24 M. Kijak, K. Nawara, A. Listkowski, N. Masiera, J. Buczyńska, N. Urbańska, G. Orzanowska, M. Pietraszkiewicz and J. Waluk, 2+2 Can Make Nearly a Thousand! Comparison of Di- and Tetra-Meso-Alkyl-Substituted Porphycenes, *J. Phys. Chem. A*, 2020, **124**, 4594–4604.

25 B. Holmquist, Magnetic circular dichroism, *Methods Enzymol.*, 1986, **130**, 270–291.

26 M. J. Frisch, G. W. Trucks, H. B. Schlegel, G. E. Scuseria and M. A. Robb, *et al.*, *Gaussian 16, Revision A.03*, Gaussian, Inc., Wallingford CT, 2016.

27 G. te Velde, F. M. Bickelhaupt, E. J. Baerends, C. Fonseca Guerra, S. J. A. van Gisbergen, J. G. Snijders and T. Ziegler, Chemistry with ADF, *J. Comput. Chem.*, 2001, **22**, 931–967.

28 S. Sripothongnak, C. J. Ziegler, M. R. Dahlby and V. N. Nemykin, Controllable and Reversible Inversion of the Electronic Structure in Nickel N-Confused Porphyrin: A Case When MCD Matters, *Inorg. Chem.*, 2011, **50**, 6902–6909.

29 C. J. Ziegler, N. R. Erickson, M. R. Dahlby and V. N. Nemykin, Magnetic Circular Dichroism Spectroscopy of N-Confused Porphyrin and Its Ionized Forms, *J. Phys. Chem. A*, 2013, **117**, 11499–11508.

30 G. A. Peralta, M. Seth and T. Ziegler, Magnetic circular dichroism of porphyrins containing M = Ca, Ni, and Zn. A Computational study based on time-dependent density functional theory, *Inorg. Chem.*, 2007, **46**, 9111–9125.

31 M. Gouterman, Spectra of porphyrins, *J. Mol. Spectrosc.*, 1961, **6**, 138–163.

32 J.-L. Soret, Analyse spectrale: Sur le spectre d'absorption du sang dans la partie violette et ultra-violette, *C. R. Acad. Sci.*, 1883, **97**, 1269–1270.

33 F. Santoro, A. Lami, R. R. Improta, J. Bloino and V. Barone, Effective method for the computation of optical spectra of large molecules at finite temperature including the Duschinsky and Herzberg–Teller effect: The Q_x band of porphyrin as a case study, *J. Chem. Phys.*, 2008, **128**, 224311.

34 B. Minaev, Y. H. Wang, C. K. Wang, Y. Luo and H. Ågren, Density functional theory study of vibronic structure of the first absorption Q band in free-base porphin, *Spectrochim. Acta, Part A*, 2006, **65**, 308–323.

35 P. Kowalska, M. D. Peeks, T. Roliński, H. L. Anderson and J. Waluk, Detection of a weak ring current in a nonaromatic porphyrin nanoring using magnetic circular dichroism, *Phys. Chem. Chem. Phys.*, 2017, **19**, 32556–32565.

17950 | *Phys. Chem. Chem. Phys.*, 2024, **26**, 17944–17950

This journal is © the Owner Societies 2024